



## ORIGINAL RESEARCH

# The effect of nitrogen source and levels on hybrid aspen tree physiology and wood formation

Anna Renström<sup>1</sup> | Shruti Choudhary<sup>1</sup> | Madhavi Latha Gandla<sup>2</sup> | Leif J. Jönsson<sup>2</sup> |  
 Mattias Hedenström<sup>2</sup> | Sandra Jämtgård<sup>1,3</sup> | Hannele Tuominen<sup>1</sup>

<sup>1</sup>Umeå Plant Science Centre, Department of Forest Genetics and Plant Physiology, Swedish University of Agricultural Sciences, Umeå, Sweden

<sup>2</sup>Department of Chemistry, Umeå University, Umeå, Sweden

<sup>3</sup>Department of Forest Ecology and Management, Swedish University of Agricultural Sciences, Umeå, Sweden

## Correspondence

Anna Renström,  
 Email: [anna.renstrom@slu.se](mailto:anna.renstrom@slu.se)

## Funding information

Swedish Research Foundation Formas, Grant/Award Number: 2021-00992; Trees and Crops for the Future, Grant/Award Number: 2022.3.2.5-426; BIO4ENERGY, Grant/Award Number: B4E3-FM-2-06

Edited by B. Neuhaeuser

## Abstract

Nitrogen can be taken up by trees in the form of nitrate, ammonium and amino acids, but the influence of the different forms on tree growth and development is poorly understood in angiosperm species like *Populus*. We studied the effects of both organic and inorganic forms of nitrogen on growth and wood formation of hybrid aspen trees in experimental conditions that allowed growth under four distinct steady-state nitrogen levels. Increased nitrogen availability had a positive influence on biomass accumulation and the radial dimensions of both xylem vessels and fibers, and a negative influence on wood density. An optimal level of nitrogen availability was identified where increases in biomass accumulation outweighed decreases in wood density. None of these responses depended on the source of nitrogen except for shoot biomass accumulation, which was stimulated more by treatments complemented with nitrate than by ammonium alone or the organic source arginine. The most striking difference between the nitrogen sources was the effect on lignin composition, whereby the abundance of H-type lignin increased only in the presence of nitrate. The differential effect of nitrate is possibly related to the well-known role of nitrate as a signaling compound. RNA-sequencing revealed that while the lignin-biosynthetic genes did not significantly (FDR <0.01) respond to added  $\text{NO}_3^-$ , the expression of several laccases, catalysing lignin polymerization, was dependent on N-availability. These results reveal a unique role of nitrate in wood formation and contribute to the knowledge basis for decision-making in utilizing hybrid aspen as a bioresource.

## KEYWORDS

H-type lignin, lignin composition, N-nutrition, organic vs. inorganic N, *Populus tremula* x *P. tremuloides*, Pyrolysis-GC/MS, xylogenesis

## 1 | INTRODUCTION

Nitrogen (N) fertilization is a common practice to boost net primary production, especially in terrestrial ecosystems suffering from N limitation. In boreal forests, N fertilization can increase severalfold the volume

production of trees (Bergh et al. 1999). Also, short-rotation plantations of various poplar and willow species gain significant increases in biomass production when fertilized with N (Rodrigues et al. 2021). The downside of fertilization is leaching of N to the surrounding environment and the risks of nutrient imbalance in aquatic systems

This is an open access article under the terms of the [Creative Commons Attribution](https://creativecommons.org/licenses/by/4.0/) License, which permits use, distribution and reproduction in any medium, provided the original work is properly cited.

© 2024 The Authors. *Physiologia Plantarum* published by John Wiley & Sons Ltd on behalf of Scandinavian Plant Physiology Society.

(Canfield et al. 2010). To avoid the overuse of fertilizers, we need better knowledge on the effects of N on both qualitative and quantitative properties of angiosperm trees such as *Populus* sp.

It is well established that N increases tree volume production by stimulating the activity of the vascular cambium through an unknown mechanism that most likely includes cytokinins (Aloni 2021). Functional studies with cytokinin biosynthetic and catabolic genes in both *Arabidopsis thaliana* and hybrid aspen supported the role of cytokinins in the regulation of cambial activity (Matsumoto-Kitano et al. 2008; Nieminen et al. 2008; Immanen et al. 2016), but the link to N status of the plants was not studied. Nitrogen also influences the basic density of wood. Increased N availability reduced wood density in poplar (Luo et al. 2005; Hacke et al. 2010), most probably as a consequence of increased growth rate (Pretzsch et al. 2018). In addition to wood density, addition of N (in the form of ammonium nitrate,  $\text{NH}_4\text{NO}_3$ ) has been shown to increase vessel diameter (Hacke et al. 2010), and causes shorter and wider fibers (Pitre et al. 2007a), thinner secondary cell walls (Plavcová et al. 2013) and tension wood formation (Luo et al. 2005; Pitre et al. 2010) in poplar. These responses vary between *Populus* species of different growth rates (Li et al. 2012), necessitating further studies in these species.

Changes in xylem properties influence the hydraulic properties of the xylem. Treatment with a high  $\text{NH}_4\text{NO}_3$  concentration increased the diameter of xylem vessels as well as specific conductivity ( $K_s$ ) compared to treatment with a moderate level of  $\text{NH}_4\text{NO}_3$  in hybrid poplar (Hacke et al. 2010). Increased stem hydraulic capacity coincided with increased expression of several aquaporins that have been functionally characterized as water channels, suggesting that aquaporins mediate N-stimulated vessel expansion through increased water transport (Hacke et al. 2010).

In addition to the control of meristem activity and wood morphology, N status can influence wood chemistry. Greenhouse experiments with elevated levels of  $\text{NH}_4\text{NO}_3$  decreased both the S/G lignin ratio and lignin content compared to low levels or lack of  $\text{NH}_4\text{NO}_3$  in one specific genotype (Pitre et al. 2007b) and across 396 clonally replicated genotypes (Novaes et al. 2009) of hybrid poplar. Increased N availability has also been shown to stimulate the abundance of *p*-hydroxybenzoylated (Goacher et al. 2021) and *p*-hydroxyphenyl (Pitre et al. 2007b) lignin. Lignin changes were shown to depend on the position in the stem (Euring et al. 2014), and it seems, therefore, that N responses in wood chemistry vary depending on the level of the available N as well as the age of the trees.

Another factor influencing tree responses to N availability is the source of N (Yan et al. 2019). Nitrogen is taken up by trees as nitrate or ammonium ions depending on tree species and growth environment (Rennenberg et al. 2010; Song et al. 2015; Zhou et al. 2021). Plants can acquire N also in organic forms as amino acids or small peptides (Näsholm et al. 2009; Inselsbacher & Näsholm 2012). However, the effects of the different N sources on the physiology and wood formation of trees have not been explored yet. In this study, we established a physiologically relevant strategy to investigate the effect of four different N sources, arginine, ammonium ( $\text{NH}_4^+$ ), nitrate ( $\text{NO}_3^-$ ) and ammonium nitrate ( $\text{NH}_4\text{NO}_3$ ), at four different levels on plant growth, cambial

activity and xylem differentiation in clonally propagated hybrid aspen (*P. tremula* × *P. tremuloides*) clone T89 trees. Increasing levels of N stimulated cambial activity, reduced wood density, and increased xylem cell dimensions regardless of the N-source. However, significant differences were observed in wood chemistry depending on the source of N, which can have a bearing on the type of N to be used in forest practices.

## 2 | MATERIALS AND METHODS

### 2.1 | Plant growth and fertilization strategy

Approximately 10-cm-tall *in vitro* hybrid aspen (*Populus tremula* × *P. tremuloides*) cuttings were transplanted in 3-L pots with a soil mixture of peat:perlite (10:1) that was mixed with 2 g  $\text{L}^{-1}$  lime prior to use to increase the pH. Trees were cultivated in greenhouse for 10 weeks with 18:6 h day/night cycles, with an average daily temperature of  $\sim 22^\circ\text{C}$  and a relative humidity of 50–60%. In addition to the ambient light, trees were illuminated with Fionia FL300 Sunlight LED lamps (Senmatic A/S) with a maximal irradiance of 150–250  $\mu\text{mol m}^{-2} \text{s}^{-1}$ . Trees were supported with stakes during their growth.

The fertilisation regime was designed to maintain a stable internal N-level in the trees by adjusting the fertilisation according to their growth. We followed the formula by (Ingestad 1979)  $N_t - N_s = N_s (e^{R_N(t-s)} - 1)$  which determines the amount of N to be added each day on the basis of the estimated N content at the start ( $N_s$ ) of the application and at each day ( $N_t$ ). Rate of increase in plant N content ( $R_N$ ) was calculated on the basis of the estimated total N content ( $\sim 1$  g) of hybrid aspen trees cultivated for 10 weeks in non-N-limiting conditions of pilot studies. Thus, ( $N_t - N_s$ ) is the calculated amount of N to be added from day *s* to day *t* to allow plant N content to follow  $R_N$ . The fertilizer was based on “Rika-S” (SW HORTO AB). The pH was adjusted with either KOH or HCl to approximately 5.6. Nitrogen was supplied in four different forms. See Table S1 for complete nutrient composition and the amounts of added N.

Two separate experiments (Experiment I and II) were performed with a slightly different steady-state fertilization regime. In experiment I, N-levels were defined as limited, sub-optimal and optimal, corresponding to approximately 0.16, 0.56 and 1.06 g of N supplied in total to each tree by the end of the experiment. The pot substrate was “Solmull” (Hasselfors Garden), which contains naturally abundant nutrients and low level of N (approximately 20 mg N per litre). After three weeks of growth without fertilization, the trees were supplemented, with one or two days intervals, with nutrient solution until the end of the experiment. Fertilizer solution was added directly to the top of the soil and the potential runoff was captured by trays placed underneath each pot. The soil was kept humid by adding water to the trays to prevent potential nutrient runoff.

In Experiment II, the saplings were potted to the same pot substrate as in Experiment I, but this time supplemented to contain 40 mg N per liter (either in the form of arginine,  $\text{NH}_4^+$ ,  $\text{NH}_4\text{NO}_3$  or  $\text{NO}_3^-$ ) to avoid initial plant stress due to low N level. This increased the total amount of N applied to each tree. Thus, in Experiment II,

the N-levels were assigned as sub-optimal, optimal, and excessive, corresponding to a total N-addition of 0.56 g, 1.12 g and 1.68 g, respectively. The residual N content in the soil at the end of the experiment II was  $0.0055 \pm 0.0001$  g in the suboptimal,  $0.0194 \pm 0.0098$  g in the optimal, and  $0.1155 \pm 0.0295$  g in the excessive N conditions, indicating that most of the applied N was taken up by the trees.

The results are presented in main figures for Experiment I and in supplemental figures for Experiment II. Experiment I took place in the summer and Experiment II in the late autumn, which is probably the reason for the differences in the overall growth rate of the trees in the two different experiments. RNA sequencing, saccharification and root biomass results pertain only to Experiment I, while all other analyses were performed for material collected from both experiments. Raw data for both experiments is shown in Table S1.

## 2.2 | Analyses of tree growth and physiological parameters

Stem height and diameter at the base of the tree were measured on a weekly basis. At the end of the experiment, after 10 weeks of growth, fresh weight of the shoot and roots was recorded. The dry weight of wood was estimated according to the formula  $1/3 \times \pi \times \text{stem height} \times (\text{stem diameter}/2)^2 \times \text{wood density}$  (Escamez et al. 2017). Instantaneous gas-exchange measurement was made on a mid-stem leaf at the end of the experiment using a LI-6400XT (LI-COR Biosciences, Inc.). Parameter settings used for the LI-6400XT were: flow rate  $250 \mu\text{mol s}^{-1}$ ,  $\text{CO}_2$  reference  $380 \mu\text{mol mol}^{-1}$ , Tleaf  $25^\circ\text{C}$  and PAR  $800 \mu\text{mol m}^{-2} \text{s}^{-1}$ .

For carbon (C) and N analysis, three newly expanded leaves were collected at the end of the experiment. C- and N-analysis was done on dried, milled leaves with Elemental Analyzer Isotope Ratio Mass Spectrometry (EA-IRMS) at the SLU Stable Isotope Laboratory. The instrument setup consisted of an elemental analyser (Flash EA 2000, Thermo Fisher Scientific) connected to a continuous flow isotope ratio mass spectrometer (DeltaV, Thermo Fisher Scientific), which allowed detection of C- and N-content and the isotopic composition of these elements.

The  $^{13}\text{C}/^{12}\text{C}$  isotopic composition in planta is usually lower than in the atmosphere since the kinetics of  $\text{CO}_2$  incorporation discriminate against the heavier isotope. The discrimination is related to the rate of water loss (decreased duration/abundance of water retention in the leaves increasing the  $^{13}\text{C}$  discrimination), and the  $^{13}\text{C}/^{12}\text{C}$  ratio can therefore be used as a proxy for plant water-use efficiency (Farquhar et al. 1989).

## 2.3 | Wood density, chemistry and anatomy

Samples for measurement of wood density were taken 5–10 cm from the base of the stem and assessed using the water displacement method whereby a newly harvested and debarked wood sample was submerged under water in a flask placed on a balance. The weight of

water (in grams at room temperature) displaced by the sample corresponds to the volume of the sample (in  $\text{cm}^3$ ). Dry weight of the sample was obtained after drying in oven for two days at  $50^\circ\text{C}$ . Wood density was calculated as dry weight of wood divided by the volume of wood.

Stem pieces for wood chemistry assessment were collected 10–20 cm from the base of the stem. The stem pieces were debarked, and differentiating xylem layers were removed by scraping from the surface of the stem. The remaining mature part of the wood was freeze-dried and, after removal of the pith and the leaf traces, ball-milled into a fine powder. Extractives were removed from the wood powder according to Gandla et al. (2015). Extractive-free, ball-milled wood powder ( $50 \mu\text{g} \pm 10 \mu\text{g}$ ) was applied to a pyrolyzer equipped with an autosampler (PY-2020iD and AS-1020E, Frontier Lab) connected to a GC/MS (7890A/5975C; Agilent Technologies). The pyrolysis-GC/MS (Py-GC/MS) conditions were the same as in Gerber et al. (2012). The pyrolysate was separated and analysed. Py-GC/MS provides sensitive chemical fingerprints whereby the contents of carbohydrates, lignin subunits (S, G, H), total lignin, other phenolic compounds, and unidentified compounds in the secondary cell walls are derived as a signal% of the integrated GC peak area (Gerber et al. 2012). *p*-hydroxybenzoylated (pHB) lignin was identified on the basis of the fragmentation pattern of *p*-hydroxybenzoic acid (base peak  $m/z$  121 (100), 138 (80), 93 (26), 65 (25), 39 (20), 43 (14), 55 (10), 63 (8), 122 (7), 53 (6)) (Faix et al. 1990). Even though the values obtained with the Py-GC/MS method are not absolute and influenced by the sensitivity of the instrument for the different compounds, they are proportional to weight%. In this study, all samples were run at the same time, allowing detection of even small differences between the relative levels of the cell wall components. The same starting material as for Py-GC/MS was used for quantification of cell wall monosaccharides from hemicelluloses and amorphous cellulose by acidic methanolysis followed by trimethylsilyl (TMS) derivatization according to Gandla et al. (2015).

Wood anatomy samples were taken 20–25 cm from the base of the stem. The tissues closest to the pith were excluded from the anatomy analysis. Sections were cut with Vibratome VT100 (Leica Microsystems) at a thickness of  $30 \mu\text{m}$ . Radial sections were always taken above the node. Eight pictures per section were taken with Leica Dmi8 microscope with colour Leica DFC 7000 T colour camera and LasX software (Leica Microsystems). Sections were stained with 0.05% Toluidine blue O and imaged in bright field mode. Images were then processed in ImageJ2 version 2.14.0/154f by the “analyze particle” function counting numbers of vessels, fibers and their lumen area. The macros for these analyses can be found in Table S1.

## 2.4 | NMR spectroscopy

Lignin was extracted from pre-grounded wood powder (the same as for Py-GC/MS) according to Mottiar et al. (2023). In short, extractives were removed by washing with ethanol and acetone. Extractive-free wood powder was ball-milled and enzymatically treated with cellulase (Cellulase “Onozuka” RS, Yakult Pharmaceutical Industry Co., Ltd.) to remove carbohydrates. The residual enzyme-lignin was rinsed and

freeze-dried. Enzyme-lignin powder (12–15 mg) was added to 5 mm NMR tubes followed by addition of 550  $\mu\text{L}$  of a 4:1 dms $\text{-d}_6$ :pyridine- $\text{d}_5$  mixture and thorough mixing. 2D  $^1\text{H}$ - $^{13}\text{C}$  Heteronuclear Single Quantum Coherence NMR experiments (HSQC) were recorded on a Bruker 850 MHz Avance III HD spectrometer equipped with a cryo-TCI probe, using the hsqcetgpsisp2.2 pulse sequence. All experiments were performed at 298 K using a relaxation delay of 0.75 s and by recording 40 transients for each of the 196 data-points in the indirect dimension. Processing was performed using Gaussian window functions with GB 0.001 in both dimensions, and LB  $-0.1$  Hz in F2 and  $-1$  Hz in F1. Peaks in the aromatic region originating from syringyl (S), guaiacyl (G), *p*-hydroxyphenyl (H) and *p*-hydroxybenzoyl units (pHB) were integrated and used for calculating the relative amounts according to Mottiar et al. (2023). Processing was performed in Topspin 3.6 (Bruker Corp.).

## 2.5 | Saccharification

The remaining stem parts from the harvest (i.e., after samples were collected for anatomy, wood chemistry and RNA analysis) were peeled and oven-dried. After drying, the stems were homogenized with a centrifugal mill (Retsch), and the 100–500  $\mu\text{m}$  particle size fraction was collected and used for saccharification with and without a pretreatment according to Gandla et al. (2021). Briefly, the dry wood fraction [50 mg; solids loading of 5% (w/w)] of each sample was subjected to analytical scale saccharification after moisture analysis (HG63 moisture analyser, Mettler-Toledo). Acid pretreatment (1% w/w sulfuric acid per gram of total reaction mixture) was performed using an Initiator single-mode microwave instrument (Biotage Sweden AB). The solid residue after acid pretreatment was separated from the hemicellulosic hydrolysate (Pretreatment liquid; PL) by centrifugation (20600 g, 15 min; Eppendorf) and subjected to enzymatic saccharification (solids loading of 5% (w/w)) after washing sequentially twice with deionized MilliQ water and twice with sodium citrate buffer (pH 5.2, 50 mM). The enzymatic saccharification was performed using liquid enzyme preparation of 5 mg of Cellic CTec-2 (Sigma-Aldrich) for 72 h at 45°C in an orbital shaking incubator with a shaking speed of 170 rpm (Ecotron incubator shaker). Samples were collected 2 and 72 h after incubation. For the samples collected after 2 h, the glucose production rate (GPR) was determined using an Accu-Chek® Aviva glucometer (Roche Diagnostics Scandinavia AB) after calibration with a set of glucose standard solutions. For the samples collected after 72 h, monosaccharide sugar yields (arabinose, galactose, glucose, xylose, and mannose) were determined using an Ion Chromatography System ICS-5000 high-performance anion-exchange chromatography system (HPAEC) with pulsed amperometric detection (Dionex; Tang et al., 2022).

## 2.6 | Statistical analyses

Statistical analysis was performed in R version 4.2.2 (2022-10-31) and RStudio version 2023.03.0 + 386. Growth response, wood anatomy and wood chemistry were all analysed using two-way ANOVA (aov

function) with N-source and N-level as factors, followed by Tukey's 'Honest Significant Difference' method (TukeyHSD function). PCA analysis was performed to reduce the dimensionality of multivariate data (prcomp function). PCA results were then visualized using a PCA-biplot (fviz\_pca\_biplot function) where both individual trees and response variables are shown in relation to the dimensions. Correlation matrix was calculated using the 'rcorr' function and 'Hmisc' package. Pearson's correlation coefficients and p-values from the correlation matrix was used in 'corrplot' function and 'corrplot' package R-studio version 2023.06.0 + 421.

## 2.7 | RNA sequencing and data analysis

A stem piece (25–35 cm from the base) was peeled, and a sample collected from the exposed surface of the wood by scraping until the mature wood. Four biological replicates were included for each of the three concentrations of applied  $\text{NO}_3^-$  from Experiment I. The sample was homogenized to fine powder in liquid nitrogen using mortar and pestle. RNA extraction was done using Sigma Spectrum™ Plant Total RNA Kit followed by the on-column DNase treatment according to manufacturer's instructions. RNA was quantified with Nanodrop 1000, and the quality was assessed with an Agilent 2100 Bioanalyzer. The RIN-values ranged from 7.9 to 9.20.

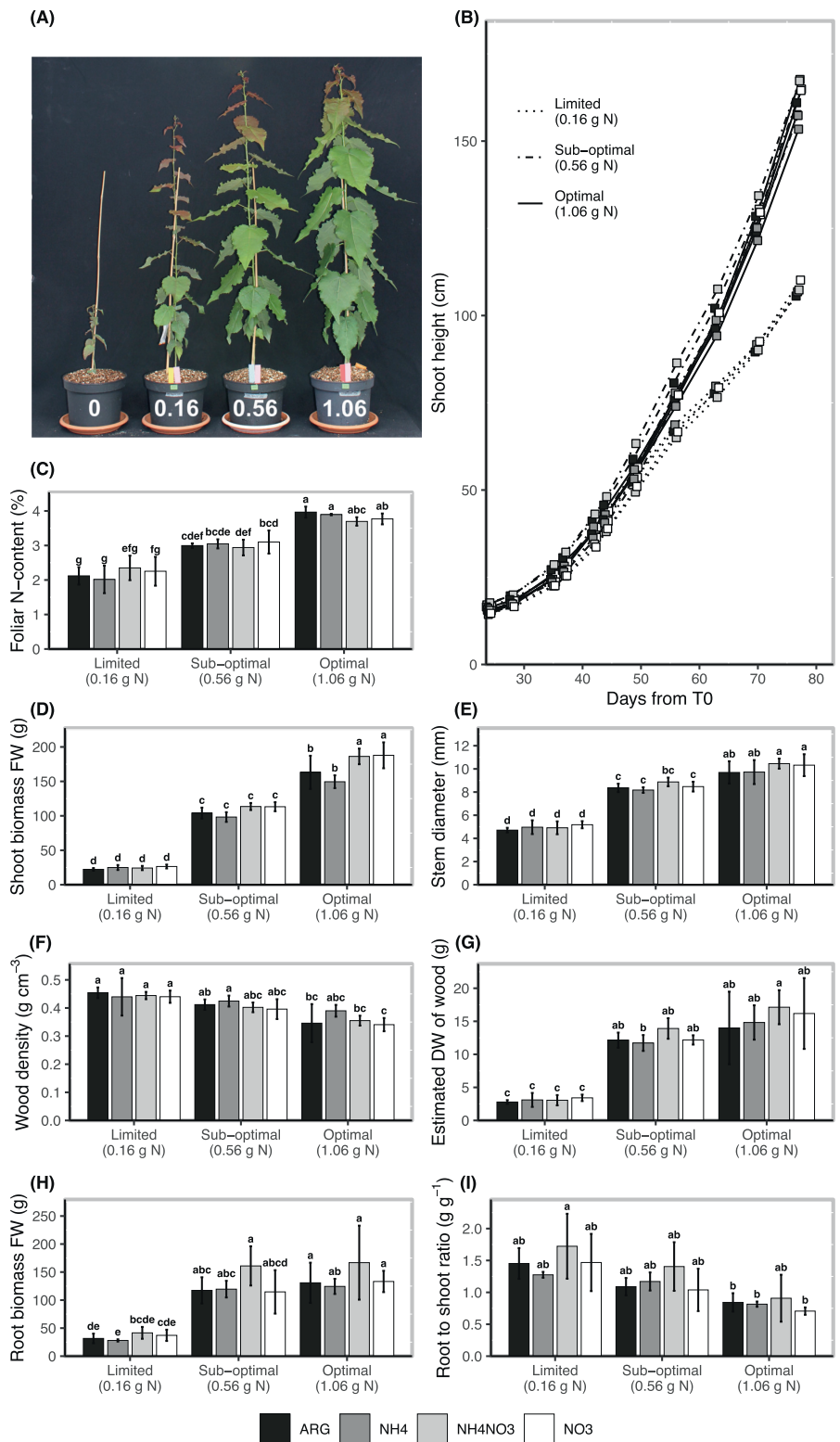
Following sequencing library generation and paired-end (2x 150 bp) sequencing using Illumina NovaSeq 6000, the raw reads were pre-processed to remove sequencing adapters using Trimmomatic (v0.39). The trimmed read pairs were quantified with Salmon (v1.9) using transcriptome index based on *P. tremula* (v2.0). After variance stabilizing transformations (VST) of the data, differential gene expression analysis was done using DESeq2 (v1.38.3) in R. Differentially expressed genes (DEGs) between the three  $\text{NO}_3^-$  concentrations were selected following the criteria of  $\log_2$  fold change (lfc)  $>1$  and a false discovery rate (FDR)  $<0.01$  (Table S3). Heatmaps were generated in R with the heatmap.2 of gplots package (v3.1.3). The gene ontology (GO) enrichments and gene co-expression networks were obtained from the respective tools available at <https://plantgenie.org/> using all genes expressed in the Aspwood database (plantgenie.org; Sundell et al. 2017) as the background. The *P. tremula* genes were annotated according to the closest *A. thaliana* homologs from TAIR or from *P. trichocarpa*.

## 3 | RESULTS

### 3.1 | The effect of the different nitrogen sources on tree biomass accumulation

Nitrogen has been shown to influence plant growth and development in different ways depending on whether it is provided in the form of  $\text{NO}_3^-$ ,  $\text{NH}_4^+$ , alone or in combination, or in organic form such as arginine (Cambui et al. 2011; Gruffman et al. 2014; Kasper et al. 2022; Lim et al. 2022). For detailed comparison of these different sources of N on wood formation of hybrid aspen trees, we

**FIGURE 1** Tree growth in response to nitrogen application. (A)  $\text{NO}_3^-$ -treated hybrid aspen trees grown for 2.5 months in the greenhouse. Trees were treated, from left to right, with 0 g, 0.16 g, 0.56 g, 1.06 g of N. Similar phenotypes were observed for all N-sources. (B) Shoot height growth. T0 indicates the start of the experiment. The points represent means.  $n = 6$ . (C) Foliar N-content in newly expanded leaves.  $n = 3$ . (D-F) Growth traits at the end of the experiment, including fresh weight of the shoot (D), stem diameter (E), wood density (F) and estimated dry weight of wood (G).  $n = 6$ . Root biomass (H) and root to shoot ratio on a fresh-weight basis (I).  $n = 3$ . Data was collected from Experiment I. Bars with error bars represent means  $\pm$  SD. Statistical significance is tested by two-way ANOVA and Tukey post-hoc test. Means not sharing any letter are significantly different at the 5% level of significance.



devised a fertilization strategy that depended on the growth rate of the trees (Ingestad 1979; Kelly & Ericsson 2003) and allowed comparison of tree growth and physiology in conditions of varying N availability (Figures 1 and S1). The addition of approximately 1 g of N was expected to be optimal based on earlier measurements of hybrid aspen trees grown for 10 weeks in optimal growth

conditions. The height growth of the trees (Figures 1B and S1B) corresponded to these expectations. Also, the foliar N-content increased steadily with increasing levels of N until it saturated at the optimal N level (Figures 1C and S1C).

Increasing availability of N increased total shoot biomass, stem height and stem diameter (Figures 1B-E and S1B-E) but decreased

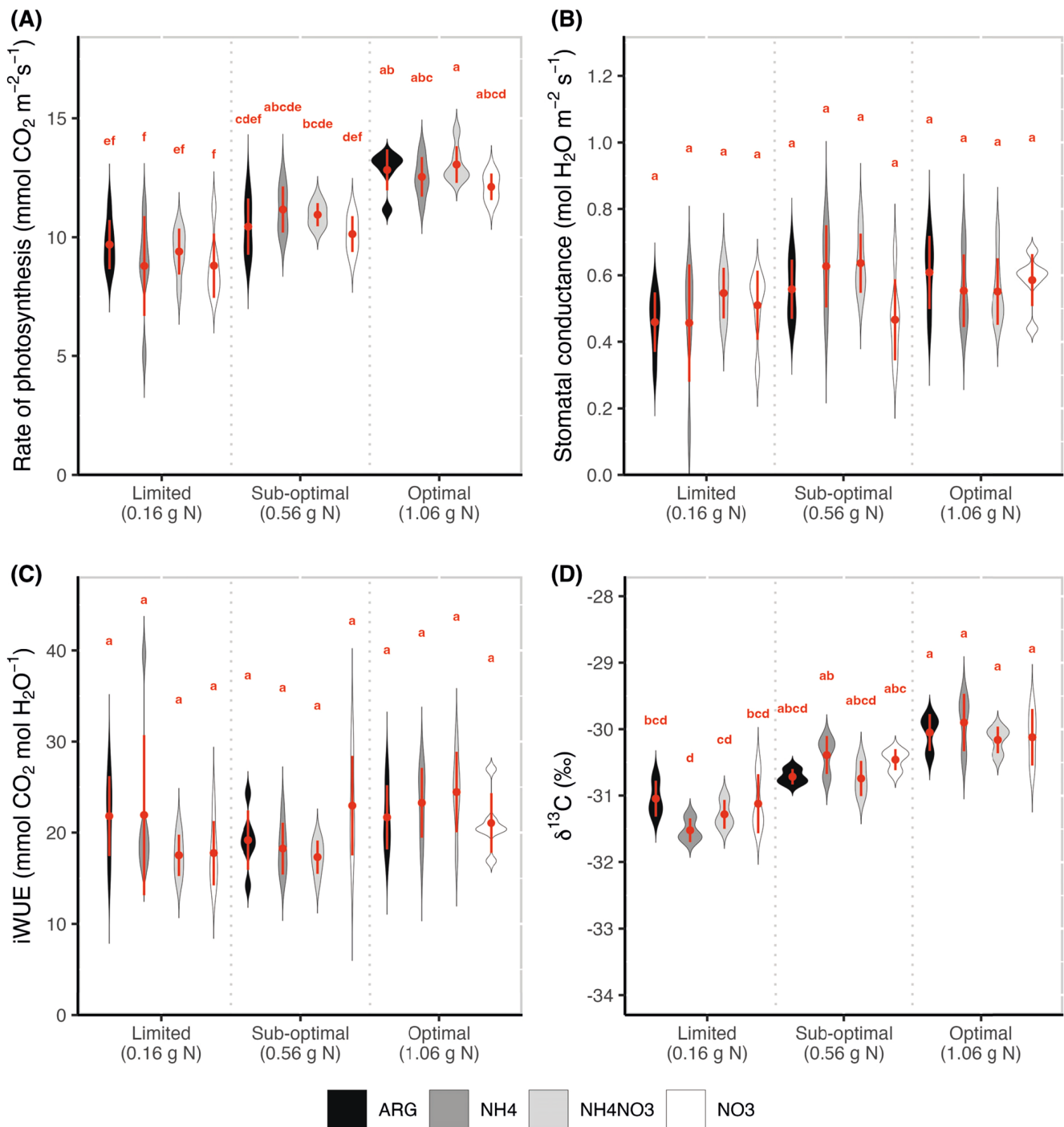


**FIGURE 2** Gas exchange and  $^{13}\text{C}$  discrimination ( $\delta^{13}\text{C}$ ) in response to nitrogen application. (A–C) Rate of photosynthesis (A), stomatal conductance (B) and instantaneous water use efficiency (iWUE) (C), analysed by gas exchange measurements with LICOR-6400XT from one mid-stem leaf.  $n = 6$ . (D)  $^{13}\text{C}$  discrimination ( $\delta^{13}\text{C}$ ).  $\delta^{13}\text{C}$ , providing an estimate of cumulative WUE, was measured by isotopic composition analysis with EA-IRMS of a newly formed leaf.  $n = 3$ . Data was collected from Experiment I. The violin plots show data distribution. Red dots and error bars indicate mean values  $\pm$  SD. Statistical significance is tested by two-way ANOVA and Tukey's HSD test. Means not sharing any letter are significantly different at the 5% level of significance.

the density of wood (Figure 1F) after 10 weeks of growth. Even though the density decreased, the estimated dry weight of the stem did not decrease but tended to increase in response to increasing N-levels (Figures 1G and 51G). The weight of the roots increased slightly while the root-to-shoot biomass ratio tended to decrease in

response to increasing N levels (Figure 1H, I). The positive effect on shoot biomass accumulation and radial growth was observed up to the optimal level of applied N. These trends were similar irrespective of the source of N, even though trees applied with arginine and  $\text{NH}_4^+$  tended to be more similar to each other than trees

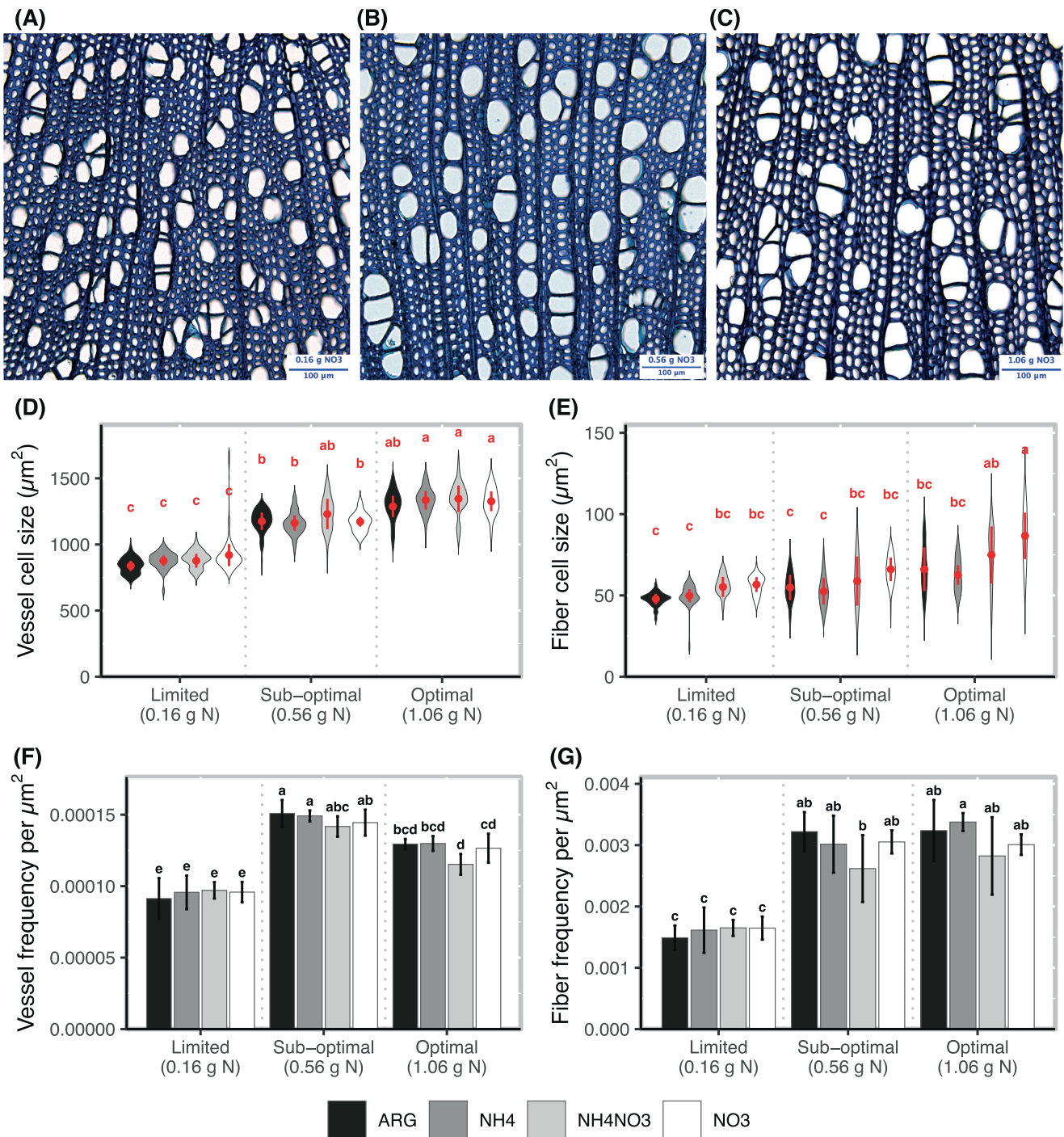


**FIGURE 3** Wood anatomy in response to nitrogen application. (A–C) Cross sections of wood from  $\text{NO}_3^-$ -treated trees in limited (A), sub-optimal (B) and optimal (C) N-conditions. (D–G) Vessel cell size (D), fiber cell size (E), vessel frequency (F), and fiber frequency (G). Xylem cell sizes and frequencies were calculated per representative area in radial sections of wood.  $n = 6$ . Data is collected from Experiment I. The violin plots show data distribution. Red dots, bars and error bars display mean values  $\pm$  SD. Statistical significance was tested by two-way ANOVA and Tukey's HSD test. Means not sharing any letter are significantly different at the 5% level of significance.

applied with  $\text{NH}_4^+$  or  $\text{NO}_3^-$  in terms of growth within the same N-level (Figures 1D, E and S1D, E). The biggest difference between the different N-sources was the higher potency of  $\text{NO}_3^-$  and  $\text{NH}_4\text{NO}_3$  than of  $\text{NH}_4^+$  or arginine to stimulate growth and in particular the total shoot biomass accumulation of the trees in the conditions of the optimal N-level (Figure 1D).

### 3.2 | The effect of nitrogen on xylem cell morphology and stem hydraulic conductivity

Instantaneous gas exchange measurements showed a tendency towards increased photosynthetic rate with increased N-level but no difference between the different N-sources within each N-level

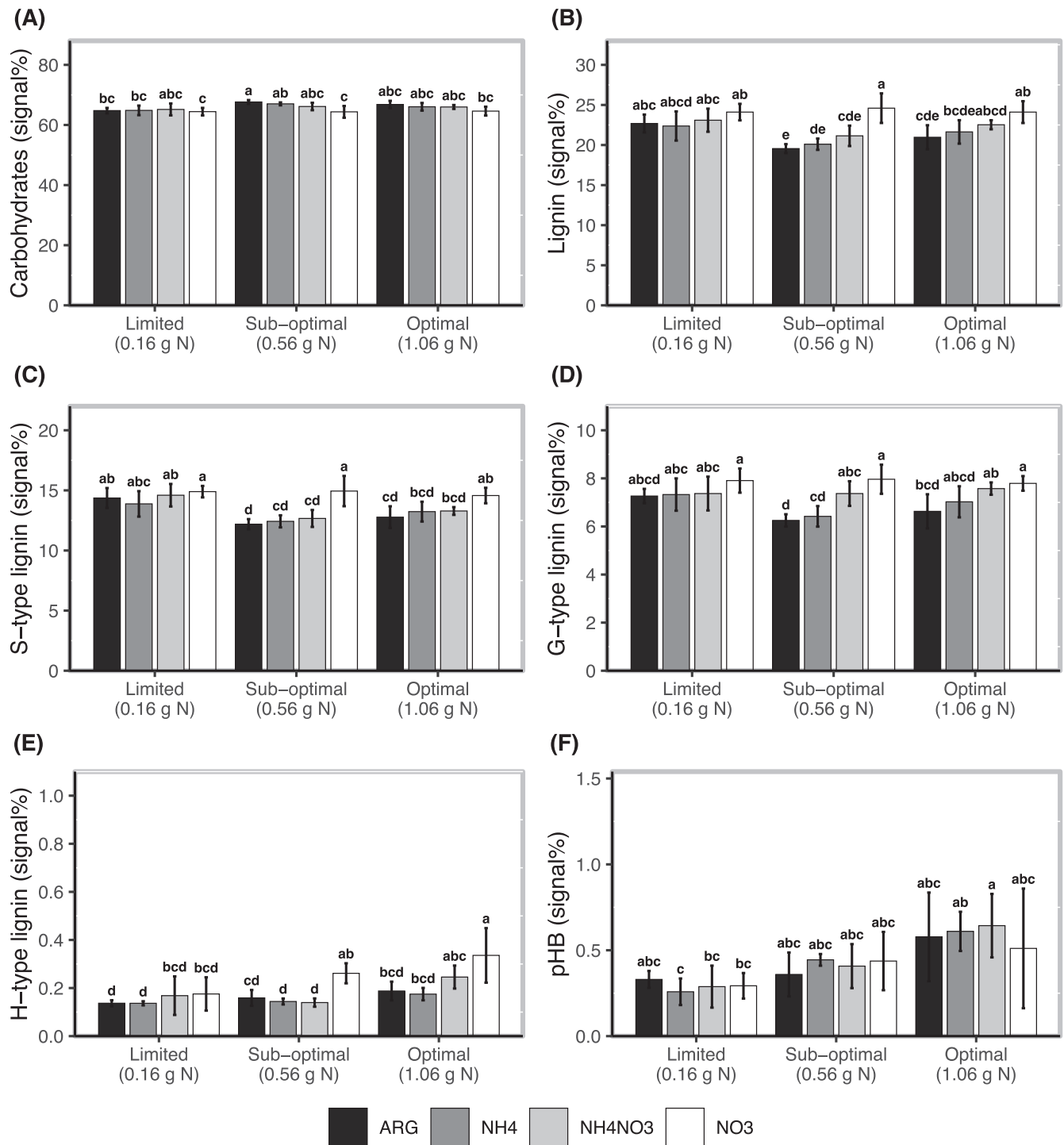


**FIGURE 4** Wood chemical composition in response to nitrogen application. (A–F) The analysis of the chemical components of wood by pyrolysis-GC/MS analysis. Relative contents are shown for carbohydrates (A), total lignin (B) S-type lignin (C), G-type lignin (D), H-type lignin (E) and pHB-lignin units (F).  $n = 6$ . Bars with error bars indicate means  $\pm$  SD. Statistical significance was tested by two-way ANOVA and Tukey's HSD test. Means not sharing any letter are significantly different at the 5% level of significance.

(Figures 2A and S2A). Instantaneous water use efficiency (iWUE) and stomatal conductance were not influenced by the source or the availability of N (Figures 2B, C and S2B, C).

Carbon discriminant analysis was used to analyse the cumulative, rather than instantaneous, effect of N. A decrease in  $^{13}\text{C}$  discrimination with increasing N-availability indicated elevated

photosynthetic efficiency even though the effect levelled off with the highest N-levels (Figures 2D and S2D). As carbon discrimination can also be used as a proxy for plant water use efficiency (Farquhar et al. 1989), the observed trends of  $^{13}\text{C}$  discrimination were indicative of increased water use efficiency in response to increased N availability.

In line with the increase in water use efficiency, the analysis of wood anatomy (Figure 3A–C) revealed that the radial dimensions of the xylem vessel elements increased with increasing N-levels, independent of the N-source (Figure 3D). Also, xylem fibers showed a tendency towards increased cell size in response to increasing N-levels (Figure 3E). The frequencies of both vessels and fibers increased from limited to sub-optimal N-level (Figure 3F, G). Neither cell frequencies nor cell sizes changed further with increasing N-availability (Figure S3).

### 3.3 | The effect of nitrogen on wood chemistry

The effect of the different N-sources was studied on wood chemistry by Py-GC/MS (Table S2), which provides an estimate of the relative contents of the cell wall chemical components (Gerber et al. 2012). The relative content of carbohydrates did not change in any of the N conditions (Figures 4A and S4A). The relative content of total lignin as well as S- and G-type lignin decreased slightly from limited to suboptimal N-level for all N-sources except for  $\text{NO}_3^-$  (Figures 4B–D and S4B–D). In  $\text{NO}_3^-$ -treated trees, however, lignin content did not decrease in response to increasing  $\text{NO}_3^-$ -level (Figures 4B and S4B). Most strikingly, increasing levels of  $\text{NO}_3^-$  and, to a lesser extent,  $\text{NH}_4\text{NO}_3$  increased the relative content of H-lignin (Figures 4E and S4E). *p*-hydroxybenzoylated lignin levels tended to increase with increasing N-levels for all N-sources (Figures 4F and S4F). NMR analysis revealed similar results for the levels and composition of lignin in a subset of  $\text{NO}_3^-$ -treated trees (Table S1).

Saccharification efficiency was analysed in conditions of limited, sub-optimal and optimal N availability to analyse whether changes in lignin content influence feedstock processability in our conditions. There were no statistically significant differences in saccharification yields of any of the sugars (glucose, xylose, mannose, arabinose, galactose) after mild acidic pretreatment. Without the pretreatment, the release of xylose increased slightly with increasing N-level but statistically significantly only for the arginine treatment (Table S1). The potential influence of wood hemicelluloses on the saccharification efficiency was excluded on the basis of wood monosaccharide composition that did not differ between either N-sources or N-levels (Table S1).

### 3.4 | The effect of nitrate application on global gene expression

Since  $\text{NO}_3^-$  has been shown to have a signaling function in *planta*, this treatment was selected for transcriptional analysis. Transcriptome profiles from RNA-sequencing data were analysed to assess the gene expression changes in developing xylem under limited, sub-optimal and optimal  $\text{NO}_3^-$  availabilities. The PCA plot, based on the normalized gene counts, showed a clear separation of samples treated with limited  $\text{NO}_3^-$  from sub-optimal and optimal ones that grouped together (Figure 5A). The GO analysis presented significant enrichment of ‘oxidation–reduction process’ among the upregulated and the ‘transcription factor complex’ among the downregulated differentially expressed genes (DEGs) in optimal  $\text{NO}_3^-$  conditions (Figure 5B). The differential gene expression analysis

showed a total of 832 DEGs (FDR <0.01) between three pairwise comparisons (a higher  $\text{NO}_3^-$  vs a lower  $\text{NO}_3^-$ -level) (Figure 5C; Table S3). The spatial expression pattern of the DEGs that were common for the pairwise comparisons varied across the secondary vascular tissues in the AspWood database, suggesting that many processes of wood formation were affected by changes in N availability (Figure 5C). For instance, *MYB-like* helix-turn-helix transcription factor (Potra2n16c29671) was upregulated in all three pairwise comparisons and could be involved in  $\text{NO}_3^-$ -mediated lignification based on its AspWood expression in the transition zone between xylem cell wall formation and cell death (Figure 5C). Three genes homologous to the *A. thaliana* YELLOW STRIPE-LIKE 3 (YSL3) were likewise upregulated in all pairwise comparisons. *A. thaliana* YSL3 is a plasma membrane-localised metal transporter (Chu et al. 2010) that was shown to be  $\text{NO}_3^-$ -induced in an earlier study (Poovaiah et al. 2019). Further support for the connection between YSL3 and  $\text{NO}_3^-$  was provided by co-expression of the YSL3 homologs with oligopeptide transporters (OPT) and a nitrate transporter family member (NPF2.11) (Table S3).

Significant changes were observed in the expression of key  $\text{NO}_3^-$  sensing, signaling, assimilation, and transporter genes, including homologs of the *A. thaliana* NIN LIKE PROTEIN 2 (NLP2), NITRILASE 4 (NIT4), NITRITE REDUCTASE 1 (NIR1), NITRATE REDUCTASE 2 (NR2) and nitrate transporters NPF7.1 and PTR3 (Figure 5D). Although NIN LIKE PROTEIN 7 (NLP7), recently identified as a  $\text{NO}_3^-$  sensor (Liu et al. 2022), did not show any significant change, 20 potential targets of NLP7 were found among the DEGs, including NIR, LIK1, MTP10, OSCA1.5, MLKL1 and MTP10 (Table S3).

The possible role of cytokinins in  $\text{NO}_3^-$  signaling and cambial activity was supported by increased expression of the cytokinin-biosynthetic isopentenyltransferases (*IPT5a*, *5b*, and *6b*) in response to increasing  $\text{NO}_3^-$  level (Figure 5E).

The effect of  $\text{NO}_3^-$  on cell expansion has been proposed to be mediated by induction of the expression of aquaporin family genes (Hacke et al. 2010), and seven aquaporin genes displayed significant expression changes across the three  $\text{NO}_3^-$  concentrations in our RNAseq data (Figure 5F).

Among the lignin-biosynthetic machinery, significant changes were evident for the laccases LAC2, 4, 6, 11 and 17, but not for any of the lignin-biosynthetic genes (Figure 5E). However, most of the lignin-biosynthetic genes, including HCT1 and C3H3 that act in the branch-point towards G and S-type lignin biosynthesis, showed trends of lower expression in the optimal  $\text{NO}_3^-$  level compared to the suboptimal and limited levels, while CSE2 and CCoAOMT1 and 2 as well as the *pHBMT* acyltransferases, involved in lignin *p*-hydroxybenzoylation, showed the opposite trends (Figure 6).

## 4 | DISCUSSION

### 4.1 | Nitrogen in the form of nitrate surpasses other N-sources in stimulating tree biomass accumulation

The type of N-source available to the plants influences N assimilation and plant growth. The organic forms have energetic assimilation

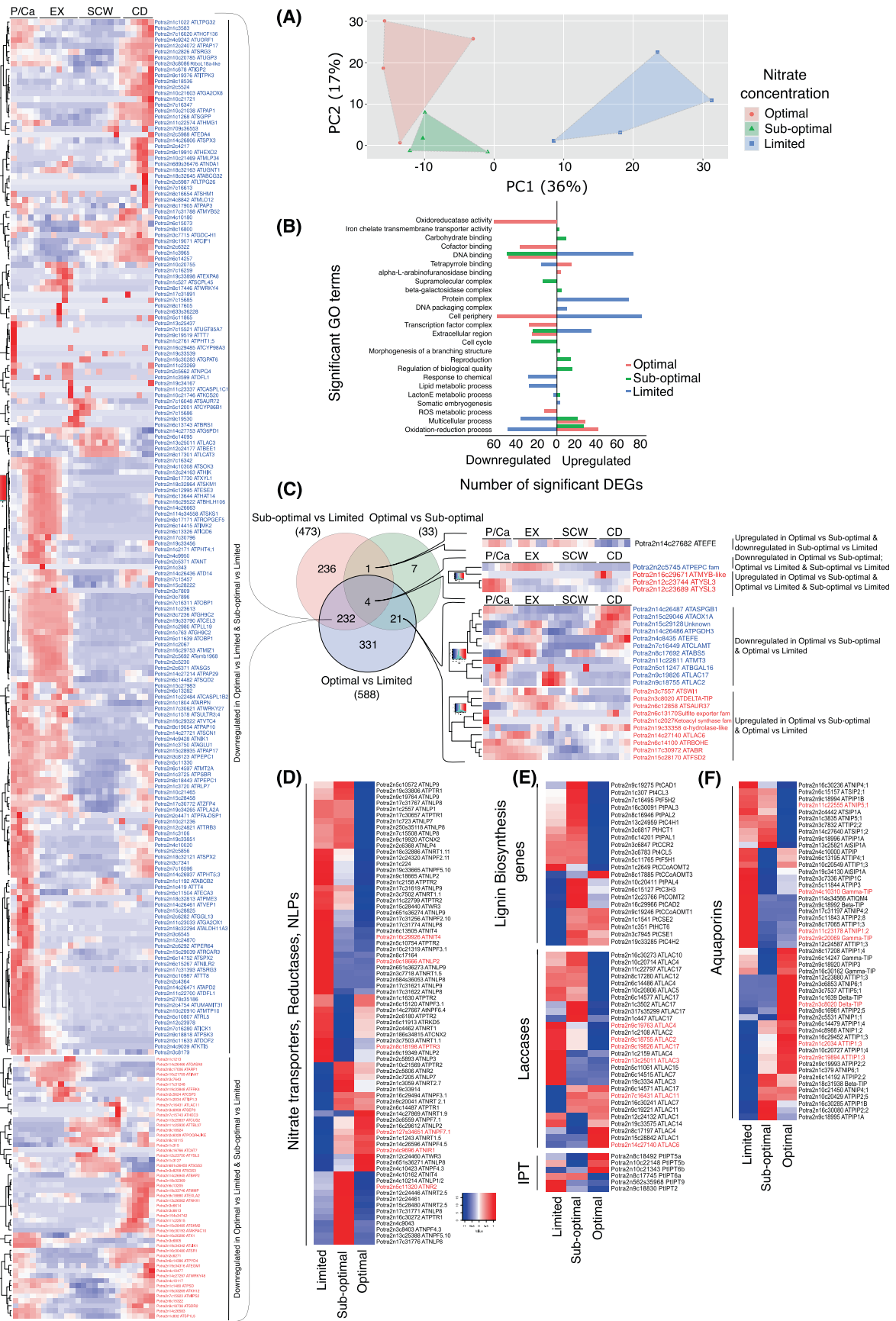


FIGURE 5 Legend on next page.

advantages over inorganic N (Franklin et al. 2017). Nitrogen is also, at least in boreal forest soils, mostly available in organic form (Inselsbacher & Näsholm 2012). On the other hand, plant species seem to differ in their preference for the N form they take up (Scott & Rothstein 2011). In the current work, the N-source had an influence on tree growth and wood properties, even though it was less pronounced than the effect of the N-level (Figure S5A-B). The organic N, applied in the form of arginine, stimulated growth and biomass accumulation of the hybrid aspen trees but less than the inorganic N forms of  $\text{NH}_4\text{NO}_3$  and  $\text{NO}_3^-$  (Figures 1 and S1). The effect of arginine was similar to the effect of  $\text{NH}_4^+$ , another positively charged N-form (Figure 1C-D). Similar results were earlier obtained in *Populus x canescens*, where shoot growth was stimulated more by the inorganic  $\text{NH}_4\text{NO}_3$  than the organic N-source of phenylalanine (Jiao et al. 2018).

A well-documented effect of organic N is the influence on plant biomass partitioning and stimulation of biomass accumulation primarily in the roots, which leads to an increased root-to-shoot ratio compared to inorganic N sources (Cambui et al. 2011; Franklin et al. 2017). This may be due to the direct incorporation of organic N into the roots (Cambui et al. 2011) or differences in the cost of assimilation in different plant parts (Franklin et al. 2017). Therefore, the question arises whether, in our experiments, the lower biomass stimulation of shoots by arginine, compared to  $\text{NO}_3^-$  and  $\text{NH}_4\text{NO}_3$ , was due to preferential accumulation of root biomass in response to arginine. Arginine did, however, not increase the root growth of hybrid aspen trees compared to the inorganic N-sources (Figure 1H). Organic N has been shown to primarily stimulate the rooting of young seedlings (Lim et al. 2022), and it is possible that the inability of arginine to stimulate root growth in our experiments was due to the fact that we used *in vitro*-propagated saplings that had pre-formed roots before exposure to the different N conditions in the soil. It is also possible that arginine and  $\text{NH}_4^+$  are less accessible to the roots due to their positive charge and, hence, attraction to the negatively charged surfaces of organic soil particles, as proposed earlier (Inselsbacher et al. 2011; Lim et al. 2022). In any case, in our experimental conditions, it is the  $\text{NO}_3^-$  complemented, inorganic forms that seem to stimulate biomass accumulation more than the organic N-source in hybrid aspen trees.

Increased biomass accumulation is commonly associated with decreased wood density (Lindström 1996; Luo et al. 2005; Hacke et al. 2010). In our experimental setup, all measured biomass-related traits showed increases in response to increasing N-level, independent of the source of N, up to the application level of 1 g per tree (Figures 1 and S1). In the same range of increasing N levels, wood

density decreased in the tree stem (Figure 1F), confirming the frequently observed negative relationship between biomass accumulation and wood density also in our experimental conditions. Consequently, wood density correlated negatively with N-level as well as leaf N-content (Figure S6). Interestingly, even though wood density decreased with increasing N-level, the overall biomass accumulation on a dry weight basis continued to increase (Figures 1G and S1G), supporting the potential of increased nitrogen availability in stimulating biomass accumulation without a drastic negative impact on wood density in hybrid aspen trees.

## 4.2 | Water transport and use efficiency are influenced by nitrogen level

Stems' hydraulic conductivity can be estimated theoretically according to the Poiseuille equation according to which the volumetric flow of water is proportional to the 4th power of the radius of the water-conducting tubes (Tyree & Ewers 1991). This means that the diameter of the vessel elements has a significant influence on water transport and, hence, nutrient uptake of tree stems. Interestingly, N is known to stimulate vessel expansion (Hacke et al. 2010; Plavcová et al. 2013) and, hence, increase its own uptake and transport potential along with the increase in mass flow (McMurtrie & Näsholm 2018). Increased N-level increased the diameter of the vessels also in our experiments (Figures 3 and S3) in a manner that did not depend on N-source. Increased vessel diameter correlated also with increased water-use efficiency according to the  $^{13}\text{C}$ -discriminant analysis (Figures 2D and S6). Therefore, we can conclude that N had a positive influence on the water transport capacity of our trees. On another note, the positive influence of N on water transport capacity and xylem expansion entails risk for a trade-off with xylem safety in conditions of limited water availability (Pratt & Jacobsen 2017). Increased vessel diameter makes N-fertilised trees presumably more susceptible to cavitation, and it will therefore be necessary to explore, in future experiments, the effects of N on xylem cavitation as well as drought resistance of trees.

## 4.3 | Nitrate has a unique influence on lignin accumulation and composition

Lignification is a developmentally regulated process that is also influenced by biotic and abiotic stresses as well as limitations in nutrients,

**FIGURE 5** Differential gene expression in response to three  $\text{NO}_3^-$  levels. (A) Principal component analysis of RNA-sequencing data from differentiating xylem tissues of hybrid aspen trees exposed to optimal, sub-optimal and limited  $\text{NO}_3^-$ -levels.  $n = 4$ . (B) Significantly represented gene ontology (GO) terms for differentially regulated genes (DEGs). DEGs were defined on the basis of up- or downregulation in at least one of the three pairwise comparisons (optimal vs sub-optimal, optimal vs limited, sub-optimal vs limited; see Table S3 for additional information). (C) Venn diagram of up- and down-regulated DEGs (fitting the criteria of  $\text{log}_2(\text{FC}) > 1$  and  $\text{FDR} < 0.01$ ) in pairwise comparisons between the three  $\text{NO}_3^-$  levels. Heatmaps for DEGs that overlap between pairwise comparisons display their expression profile during cambial growth according to the AspWood database (Sundell et al. 2017; plantgenie.org). P/Ca, phloem/cambium; Ex, expanding xylem; SCW, secondary cell wall formation; CD, cell death. (D-F) Heatmaps for expression profiles for selected gene families, including Nitrate transporters (NRT/NPF), Nitrite reductase (NIR) Nitrate reductase (NR), and NIN-Like Proteins (NLPs) (D), lignin biosynthetic genes, laccases (LAC), and isopentenyl transferase (IPT) (E) and aquaporins (F). The DEGs are shown in red. The gene annotations in (C-F) are based on the closest *A. thaliana* gene from TAIR, except for the lignin biosynthetic and the IPT genes that are annotated according to the closest homolog in *Populus trichocarpa* (Shi et al. 2010; Immanen et al. 2016). Data was collected from Experiment I.

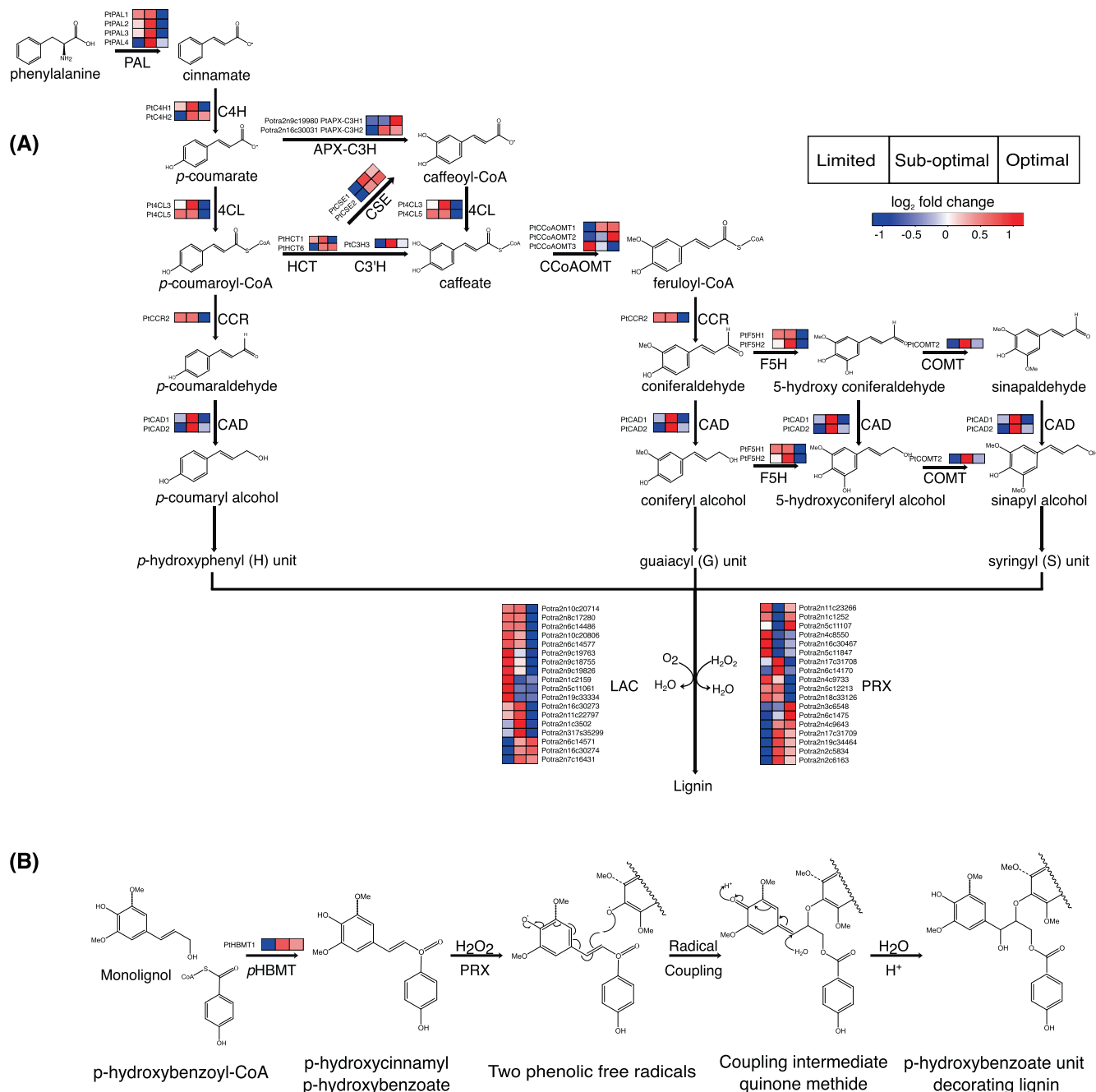


**FIGURE 6** The expression of genes involved in lignin biosynthesis and polymerization in response to three  $\text{NO}_3^-$  levels. **(A)** Lignin biosynthesis and polymerization. The monomer biosynthesis represents the dominating pathway in *Populus* according to Wang et al. (2019). The gene annotations are based on the closest homologs of the *Populus trichocarpa* (Pt) lignin-biosynthetic genes from Shi et al. (2010) and the *Populus tremula* (Potra) laccases and peroxidases from Sundell et al. (2017). Only highly expressed laccases and peroxidases (VST >3) in the secondary xylem tissues, according to the Aspwood database (plantgenie.org), are shown. **(B)** Incorporation of monolignol–pHBMT conjugates into lignin polymer. The gene annotations were based on the closest *Populus trichocarpa* (Pt) pHBMT genes from de Vries et al. (2022). PAL, L-phenylalanine ammonia-lyase; C4H, cinnamate 4-hydroxylase; C3H, 4-coumarate 3-hydroxylase; COMT, caffeic acid/5-hydroxyconiferaldehyde O-methyltransferase; F5H, ferulate-5-hydroxylase/coniferaldehyde 5-hydroxylase; 4CL, 4-coumarate:CoA ligase; HCT, *p*-hydroxycinnamoyl-CoA:quinic acid *p*-hydroxycinnamoyltransferase; C3H, 4-coumarate 3-hydroxylase; CSE, caffeoyl shikimate esterase; CCoAOMT, caffeoyl-CoA 3-O-methyltransferase; CCR, cinnamoyl-CoA reductase; CAD, cinnamyl alcohol dehydrogenase; pHBMT, *p*-hydroxybenzoyl-CoA monolignol transferase; LAC, laccase; PRX, peroxidase.

such as iron, phosphorus and N (Liu et al. 2018; Cesarino 2019; Chantréau & Tuominen 2022). Increased availability of N inhibits, in general, the lignin-biosynthetic pathway, whereas limiting N stimulates lignification (Fritz et al. 2006). In woody tissues of *Populus* trees,

increased N supply resulted in wood properties having a juvenile character with decreased lignin and S/G content (Pitre et al. 2007b). We detected, similarly, that the lignin content decreased at optimal and sub-optimal levels of N compared to limited N but did not further

decrease with excessive N-levels (Figures 4 and S4). This holds true for all N-sources tested except for  $\text{NO}_3^-$ , which did not significantly influence lignin content in any of the applied N-levels (Figures 4B and S4B). Even though increased  $\text{NO}_3^-$  availability did not influence the total lignin content, there was a clear stimulatory effect on the accumulation of the H-type lignin (Figures 4E and S4E). Also, the other  $\text{NO}_3^-$  containing N-source,  $\text{NH}_4\text{NO}_3$ , increased H-type lignin accumulation in the higher N-levels. An increase in the relative content of H-lignin was also observed by Pitre et al. (2007b) after application of high (10 mM)  $\text{NH}_4\text{NO}_3$  compared to adequate (1 mM)  $\text{NH}_4\text{NO}_3$  in hybrid poplar. The fact that H-type lignin is mainly deposited in the middle lamella and primary cell walls (Fukushima & Terashima 1990) suggests that a larger proportion of the xylem tissues were in the stage of early differentiation and/or having thinner secondary cell walls, which in turn could be due to changes in cambial activity or the spatio-temporal regulation of xylem differentiation. Increased H-lignin could also be related to H-type lignin functioning as a “stress lignin” (Lange et al. 1995; Cesarino 2019) and hence excessive  $\text{NO}_3^-$  being experienced as some kind of stress (Plavcová et al. 2013) even though it should be noted that stress-related symptoms were not observed in terms of growth penalty of the trees and that the effect was not only related to excessive  $\text{NO}_3^-$  but discernible already at optimal level.

Lignin biosynthesis is known to be transcriptionally regulated in response to N-availability both at the level of lignin monomer biosynthesis and lignin polymerization (Cooke et al. 2003; Poovaiah et al. 2019; Zhao et al. 2022). Our RNAseq analysis revealed that the lignin-biosynthetic genes did not significantly (FDR <0.01) respond to added  $\text{NO}_3^-$ . Suppression of lignin-polymerising laccases, in particular the homologs of the *A. thaliana* LAC17 and LAC2, have been linked to reduced lignification in high-N-treated plants (Plavcová et al. 2013). We also detected suppression of several homologs of the *A. thaliana* secondary cell wall-related LAC4 and 17 in the optimal and sub-optimal  $\text{NO}_3^-$  compared to the limited  $\text{NO}_3^-$ -level (Figures 5E and 6; Table S3). Interestingly, homologs of LAC6 and 11 were upregulated in the optimal  $\text{NO}_3^-$  level, and the question is whether the expression of these laccases could be related to increased deposition of H-type lignin in response to increased availability of  $\text{NO}_3^-$ . Furthermore, a MYB-like transcription factor was upregulated by increasing  $\text{NO}_3^-$  availability (Figure 5C). As MYBs are widely recognized as central regulators of lignin biosynthesis, it is possible that this previously uncharacterized transcription factor is related to the specific changes observed in response to increased  $\text{NO}_3^-$  availability.

## 5 | CONCLUSIONS

Increased availability of N affected growth and wood formation of hybrid aspen trees in many ways. We observed increased diameter of xylem elements and decreased wood density in response to increasing availability of N. We also identified N-level that was optimal for biomass accumulation of the trees in our experimental conditions. Biomass accumulation was not significantly influenced by N-source

even though the  $\text{NO}_3^-$ -containing N-sources were somewhat more efficient. However, lignin composition was influenced by the N-source, as increased levels of  $\text{NO}_3^-$  had a stimulatory effect on the accumulation of H-type lignin. This is an interesting observation from an applied point of view as lignin composition is known to influence both wood pulping and bioprocessing (Ragauskas et al. 2014). H-lignin, in particular, can confer a high abundance of condensed-type linkages and decrease the degree of lignin polymerization (Ziebell et al. 2010; Sangha et al. 2014). Targeted fertilization with  $\text{NO}_3^-$ -containing compounds could be used in cases when wood with these lignin properties is desired. On the other hand, avoiding  $\text{NO}_3^-$ -containing fertilization of forest feedstocks could be advantageous for downstream applications where relatively low H-lignin content is preferred.

## AUTHOR CONTRIBUTIONS

AR, SJ and HT conceived the project. AR performed all growth experiments, collected and prepared the plant material for all analyses. MH performed the NMR analysis. MLG performed saccharification experiments under supervision of LJJ. SC analysed the RNAseq data. AR wrote the first draft of the manuscript, and all authors contributed to the writing.

## ACKNOWLEDGEMENTS

We acknowledge Junko Takahashi Schmid at the Biopolymer Analytical Platform (BAP) at UPSC/SLU (supported by Bio4Energy and TC4F), Marta Derba-Maceluch for technical assistance and analyses at the UPSC Microscopy Facility, the Stable Isotope Lab at SLU Umeå, and the UPSC in vitro and growth facility. We thank Àngela Carrió Seguí, Marta Pérez Alonso and Pal Miskolczi for help in sample preparations.

## FUNDING INFORMATION

The work was funded by the Swedish Research Foundation Formas (grant 2021-00992), Bio4Energy ([www.bio4Energy.se](http://www.bio4Energy.se), grant B4E3-FM-2-06), and Trees for the Future post doc program (diarie 2022.3.2.5-426).

## DATA AVAILABILITY STATEMENT

All raw data is included in Supplemental Table S1. The RNAseq data is available at NCBI with the project ID PRJNA975342. (<https://www.ncbi.nlm.nih.gov/bioproject/PRJNA975342>).

## ORCID

Anna Renström  <https://orcid.org/0009-0004-8104-3228>

## REFERENCES

- Aloni, R. (2021). Regulation of Cambium Activity. *Vascular Differentiation and Plant Hormones*. Springer Cham, 1. ed, pp. 199–214.
- Bergh, J., Linder, S., Lundmark, T. & Elfving, B. (1999). The effect of water and nutrient availability on the productivity of Norway spruce in northern and southern Sweden. *Forest Ecology and Management*, vol. 119 (1–3), pp. 51–62.
- Cambui, C.A., Svennerstam, H., Gruffman, L., Nordin, A., Ganeteg, U. & Näsholm, T. (2011). Patterns of plant biomass partitioning depend on Nitrogen source. *PLoS ONE*, vol. 6 (4), pp. 1–7.

- Canfield, D.E., Glazer, A.N. & Falkowski, P.G. (2010). The evolution and future of earth's nitrogen cycle. *Science*, vol. 330 (6001), pp. 192–196.
- Cesarino, I. (2019). Structural features and regulation of lignin deposited upon biotic and abiotic stresses. *Current Opinion in Biotechnology*, vol. 56, pp. 209–214.
- Chantreau, M. & Tuominen, H. (2022). Spatio-temporal regulation of lignification. *Advances in Botanical Research*, vol. 104, p. 27.
- Chu, H.H., Chiecko, J., Punshon, T., Lanzirrotti, A., Lahner, B., Salt, D.E. & Walker, E.L. (2010). Successful reproduction requires the function of Arabidopsis YELLOW STRIPE-LIKE1 and YELLOW STRIPE-LIKE3 metal-nicotianamine transporters in both vegetative and reproductive structures. *Plant Physiology*, vol. 154 (1), pp. 197–210.
- Cooke, J.E.K., Brown, K.A., Wu, R. & Davis, J.M. (2003). Gene expression associated with N-induced shifts in resource allocation in poplar. *Plant, Cell and Environment*, vol. 26 (5), pp. 757–770.
- Escamez, S., Latha Gandla, M., Derba-Maceluch, M., Lundqvist, S.O., Mellerowicz, E.J., Jönsson, L.J. & Tuominen, H. (2017). A collection of genetically engineered Populus trees reveals wood biomass traits that predict glucose yield from enzymatic hydrolysis. *Scientific Reports*, vol. 7 (1), pp. 1–11.
- Euring, D., Bai, H., Janz, D. & Polle, A. (2014). Nitrogen-driven stem elongation in poplar is linked with wood modification and gene clusters for stress, photosynthesis and cell wall formation. *BMC Plant Biology*, vol. 14 (1), pp. 1–13.
- Faix, O., Meier, D. & Fortmann, I. (1990). Thermal degradation products of wood. Gas chromatographic separation and mass spectrometric characterization of monomeric lignin derived products. *European journal of wood and wood products*, vol. 48 (7–8), pp. 281–285.
- Farquhar, G.D., Ehleringer, J.R. & Hubick, K.T. (1989). Carbon Isotope Discrimination and Photosynthesis. *Annual Review of Plant Physiology and Plant Molecular Biology*, vol. 40 (1), pp. 503–537.
- Franklin, O., Cambui, C.A., Gruffman, L., Palmroth, S., Oren, R. & Näsholm, T. (2017). The carbon bonus of organic nitrogen enhances nitrogen use efficiency of plants. *Plant Cell and Environment*, vol. 40 (1), pp. 25–35.
- Fritz, C., Palacios-Rojas, N., Feil, R. & Stitt, M. (2006). Regulation of secondary metabolism by the carbon-nitrogen status in tobacco: Nitrate inhibits large sectors of phenylpropanoid metabolism. *Plant Journal*, vol. 46 (4), pp. 533–548.
- Fukushima, K. & Terashima, N. (1990). Heterogeneity in Formation of Lignin. XIII. Formation of p-Hydroxyphenyl Lignin in Various Hardwoods Visualized by Microautoradiography. *Journal of Wood Chemistry and Technology*, vol. 10 (4), pp. 413–433.
- Gandla, M.L., Derba-Maceluch, M., Liu, X., Gerber, L., Master, E.R., Mellerowicz, E.J. & Jönsson, L.J. (2015). Expression of a fungal glucuronoyl esterase in populus: Effects on wood properties and saccharification efficiency. *Phytochemistry*, vol. 112 (1), pp. 210–220.
- Gandla, M.L., Mähler, N., Escamez, S., Skotare, T., Obudulu, O., Möller, L., Abreu, I.N., Bygdell, J., Hertzberg, M., Hvidsten, T.R., Moritz, T., Wingsle, G., Trygg, J., Tuominen, H. & Jönsson, L.J. (2021). Overexpression of vesicle-associated membrane protein PttVAP27-17 as a tool to improve biomass production and the overall saccharification yields in Populus trees. *Biotechnology for Biofuels*, vol. 14 (1), pp. 1–14.
- Gerber, L., Eliasson, M., Trygg, J., Moritz, T. & Sundberg, B. (2012). Multivariate curve resolution provides a high-throughput data processing pipeline for pyrolysis-gas chromatography/mass spectrometry. *Journal of Analytical and Applied Pyrolysis*, vol. 95, pp.
- Goacher, R.E., Mottiar, Y. & Mansfield, S.D. (2021). ToF-SIMS imaging reveals that p-hydroxybenzoate groups specifically decorate the lignin of fibres in the xylem of poplar and willow. *Holzforschung*, vol. 75 (5), pp. 452–462.
- Gruffman, L., Jämtgård, S., Näsholm, T. & Rennenberg, H. (2014). Plant nitrogen status and co-occurrence of organic and inorganic nitrogen sources influence root uptake by Scots pine seedlings. *Tree Physiology*, vol. 34 (2), pp. 205–213.
- Hacke, U.G., Plavcová, L., Almeida-Rodriguez, A., King-Jones, S., Zhou, W. & Cooke, J.E.K. (2010). Influence of nitrogen fertilization on xylem traits and aquaporin expression in stems of hybrid poplar. *Tree Physiology*, vol. 30 (8), pp. 1016–1025.
- Immanen, J., Nieminen, K., Smolander, O.-P., Kojima, M., Alonso Serra, J., Koskinen, P., Zhang, J., Elo, A., Mähönen, A.P., Street, N., Bhalerao, R.P., Paulin, L., Auvinen, P., Sakakibara, H. & Helariutta, Y. (2016). Cytokinin and Auxin Display Distinct but Interconnected Distribution and Signaling Profiles to Stimulate Cambial Activity. *Current biology*, vol. 26 (15), pp. 1990–1997.
- Ingestad, T. (1979). Nitrogen Stress in Birch Seedlings. II. N, K, P, Ca, and Mg Nutrition. *Physiologia Plantarum*, vol. 45 (1), pp. 149–157.
- Inselsbacher, E. & Näsholm, T. (2012). The below-ground perspective of forest plants: soil provides mainly organic nitrogen for plants and mycorrhizal fungi. *New Phytologist*, vol. 195 (2), pp. 329–334.
- Inselsbacher, E., Öhlund, J., Jämtgård, S., Huss-Danell, K. & Näsholm, T. (2011). The potential of microdialysis to monitor organic and inorganic nitrogen compounds in soil. *Soil Biology and Biochemistry*, vol. 43 (6), pp. 1321–1332.
- Jiao, Y., Chen, Y., Ma, C., Qin, J., Nguyen, T.H.N., Liu, D., Gan, H., Ding, S. & Luo, Z. Bin (2018). Phenylalanine as a nitrogen source induces root growth and nitrogen-use efficiency in Populus × canescens. *Tree Physiology*, vol. 38 (1), pp. 66–82.
- Kasper, K., Abreu, I.N., Feussner, K., Zienkiewicz, K., Herrfurth, C., Ischebeck, T., Janz, D., Majcherczyk, A., Schmitt, K., Valerius, O., Baus, G.H., Feussner, I. & Polle, A. (2022). Multi-omics analysis of xylem sap uncovers dynamic modulation of poplar defenses by ammonium and nitrate. *The Plant Journal*, pp. 1–22.
- Kelly, M.M. & Ericsson, T. (2003). Assessing the nutrition of juvenile hybrid poplar using a steady state technique and a mechanistic model. *Forest Ecology and Management*, vol. 180 (1–3), pp. 249–260.
- Lange, B.M., Lapierre, C. & Sandermann, H. (1995). Elicitor-induced spruce stress lignin: Structural similarity to early developmental lignins. *Plant Physiology*, vol. 108 (3), pp. 1277–1287.
- Li, H., Li, M., Luo, J., Cao, X., Qu, L., Gai, Y., Jiang, X., Liu, T., Bai, H., Janz, D., Polle, A., Peng, C. & Luo, Z.-B. (2012). N-fertilization has different effects on the growth, carbon and nitrogen physiology, and wood properties of slow- and fast-growing Populus species. *Journal of experimental botany*, vol. 63 (17), pp. 6173–6185.
- Lim, H., Jämtgård, S., Oren, R., Gruffman, L., Kunz, S. & Näsholm, T. (2022). Organic nitrogen enhances nitrogen nutrition and early growth of Pinus sylvestris seedlings. *Tree Physiology*, vol. 42 (3), pp. 513–522.
- Lindström, H. (1996). Basic density in Norway spruce. Part I. A literature review. *Wood and Fiber Science*, vol. 28 (1), pp. 15–27.
- Liu, K.H., Liu, M., Lin, Z., Wang, Z.F., Chen, B., Liu, C., Guo, A., Konishi, M., Yanagisawa, S., Wagner, G. & Sheen, J. (2022). NIN-like protein 7 transcription factor is a plant nitrate sensor. *Science*, vol. 377 (6613), pp. 1419–1425.
- Liu, Q., Luo, L. & Zheng, L. (2018). Lignins: Biosynthesis and Biological Functions in Plants. *International journal of molecular sciences*, vol. 19 (2), p. 335.
- Luo, Z. Bin, Langenfeld-Heyser, R., Calfapietra, C. & Polle, A. (2005). Influence of free air CO<sub>2</sub> enrichment (EUROFACE) and nitrogen fertilisation on the anatomy of juvenile wood of three poplar species after coppicing. *Trees - Structure and Function*, vol. 19 (2), pp. 109–118.
- Matsumoto-Kitano, M., Kusumoto, T., Tarkowski, P., Kinoshita-Tsujimura, K., Václavíková, K., Miyawaki, K. & Kakimoto, T. (2008). Cytokinins are central regulators of cambial activity. *Proceedings of the National Academy of Sciences of the United States of America*, vol. 105 (50), pp. 20027–20031.
- McMurtrie, R.E. & Näsholm, T. (2018). Quantifying the contribution of mass flow to nitrogen acquisition by an individual plant root. *New Phytologist*, vol. 218 (1), pp. 119–130.

- Mottiar, Y., Karlen, S.D., Goacher, R.E., Ralph, J. & Mansfield, S.D. (2023). Metabolic engineering of p-hydroxybenzoate in poplar lignin. *Plant Biotechnology Journal*, vol. 21 (1), pp. 176–188.
- Näsholm, T., Kielland, K. & Ganeteg, U. (2009). Uptake of organic nitrogen by plants. *The New phytologist*, vol. 182 (1), pp.31–48.
- Nieminen, K., Immanen, J., Laxell, M., Kauppinen, L., Tarkowski, P., Dolezal, K., Tähtiharju, S., Elo, A., Decourteix, M., Ljung, K., Bhalerao, R., Keinonen, K., Albert, V.A. & Ykä, H. (2008). Cytokinin signaling regulates cambial development in poplar. *Proceedings of the National Academy of Sciences of the United States of America*, vol. 105 (50), pp. 20032–20037.
- Novaes, E., Osorio, L., Drost, D.R., Miles, B.L., Boaventura-Novaes, C.R.D., Benedict, C., Dervinis, C., Yu, Q., Sykes, R., Davis, M., Martin, T.A., Peter, G.F. & Kirst, M. (2009). Quantitative genetic analysis of biomass and wood chemistry of *Populus* under different nitrogen levels. *New Phytologist*, vol. 182 (4), pp. 878–890.
- Pitre, F.E., Cooke, J.E.K. & Mackay, J.J. (2007a). Short-term effects of nitrogen availability on wood formation and fibre properties in hybrid poplar. *Trees - Structure and Function*, vol. 21 (2), pp. 249–259.
- Pitre, F.E., Lafarguette, F., Boyle, B., Pavy, N., Caron, S., Dallaire, N., Poulin, P.L., Ouellet, M., Morency, M.J., Wiebe, N., Ly Lim, E., Urbain, A., Mouille, G., Cooke, J.E.K. & MacKay, J.J. (2010). High nitrogen fertilization and stem leaning have overlapping effects on wood formation in poplar but invoke largely distinct molecular pathways. *Tree Physiology*, vol. 30 (10), pp. 1273–1289.
- Pitre, F.E., Pollet, B., Lafarguette, F., Cooke, J.E.K., Mackay, J.J. & Lapiere, C. (2007b). Effects of increased nitrogen supply on the lignification of poplar wood. *Journal of Agricultural and Food Chemistry*, vol. 55 (25), pp. 10306–10314.
- Plavcová, L., Hacke, U.G., Almeida-Rodríguez, A.M., Li, E. & Douglas, C.J. (2013). Gene expression patterns underlying changes in xylem structure and function in response to increased nitrogen availability in hybrid poplar. *Plant, Cell and Environment*, vol. 36 (1), pp. 186–199.
- Poovaiyah, C.R., Phalen, C., Sniffen, G.T. & Coleman, H.D. (2019). Growth and Transcriptional Changes in Poplar Under Different Nitrogen Sources. *Plant Molecular Biology Reporter*, vol. 37 (4), pp. 291–302.
- Pratt, R.B. & Jacobsen, A.L. (2017). Conflicting demands on angiosperm xylem: Tradeoffs among storage, transport and biomechanics. *Plant Cell and Environment*, vol. 40 (6), pp. 897–913.
- Pretzsch, H., Biber, P., Schütze, G., Kemmerer, J. & Uhl, E. (2018). Wood density reduced while wood volume growth accelerated in Central European forests since 1870. *Forest Ecology and Management*, vol. 429 (June), pp. 589–616.
- Ragauskas, A.J., Beckham, G.T., Biddy, M.J., Chandra, R., Chen, F., Davis, M.F., Davison, B.H., Dixon, R.A., Gilna, P., Keller, M., Langan, P., Naskar, A.K., Saddler, J.N., Tschaplinski, T.J., Tuskan, G.A. & Wyman, C.E. (2014). Lignin valorization: improving lignin processing in the biorefinery. *Science (New York, N.Y.)*, vol. 344 (6185), pp. 709–709.
- Rennenberg, H., Wildhagen, H. & Ehling, B. (2010). Nitrogen nutrition of poplar trees. *Plant Biology*, vol. 12 (2), pp. 275–291.
- Rodrigues, A.M., Costa, M.M.G. & Nunes, L.J.R. (2021). Short rotation woody coppices for biomass production: An integrated analysis of the potential as an energy alternative. *Current Sustainable/Renewable Energy Reports*, vol. 8 (1), pp. 70–89.
- Sangha, A.K., Davison, B.H., Standaert, R.F., Davis, M.F., Smith, J.C. & Parks, J.M. (2014). Chemical Factors that Control Lignin Polymerization. *The Journal of physical chemistry. B*, vol. 118 (1), pp. 164–170.
- Scott, E.E. & Rothstein, D.E. (2011). Amino acid uptake by temperate tree species characteristic of low- and high-fertility habitats. *Oecologia*, vol. 167 (2), pp. 547–557.
- Shi, R., Sun, Y.H., Li, Q., Heber, S., Sederoff, R. & Chiang, V.L. (2010). Towards a systems approach for lignin biosynthesis in *populus trichocarpa*: Transcript abundance and specificity of the monolignol biosynthetic genes. *Plant and Cell Physiology*, vol. 51 (1), pp. 144–163.
- Song, M.H., Zheng, L.L., Suding, K.N., Yin, T.F. & Yu, F.H. (2015). Plasticity in nitrogen form uptake and preference in response to long-term nitrogen fertilization. *Plant and Soil*, vol. 394 (1–2), pp. 215–224.
- Sundell, D., Street, N.R., Kumar, M., Mellerowicz, E.J., Kucukoglu, M., Johnsson, C., Kumar, V., Mannapperuma, C., Delhomme, N., Nilsson, O., Tuominen, H., Pesquet, E., Fischer, U., Niittylä, T., Sundberg, B. & Hvidsten, T.R. (2017). Aspwood: High-spatial-resolution transcriptome profiles reveal uncharacterized modularity of wood formation in *populus tremula*. *Plant Cell*, vol. 29 (7), pp. 1585–1604.
- Tang, C., Gandla, M.L. & Jönsson, L.J. (2022). Comparison of solid and liquid fractions of pretreated Norway spruce as reductants in LPMO-supported saccharification of cellulose. *Frontiers in Bioengineering and Biotechnology*, vol. 10 (December), pp. 1–13.
- Tyree, M.T. & Ewers, F.W. (1991). Tansley Review No. 34 The hydraulic architecture of trees and other woody plants. *New Phytologist*, vol. 119 (3), pp. 345–360.
- de Vries, L., MacKay, H.A., Smith, R.A., Mottiar, Y., Karlen, S.D., Unda, F., Muirragui, E., Bingman, C., Meulen, K. Vander, Beebe, E.T., Fox, B.G., Ralph, J. & Mansfield, S.D. (2022). pHBMT1, a BAHD-family monolignol acyltransferase, mediates lignin acylation in poplar. *Plant Physiology*, vol. 188 (2), pp. 1014–1027.
- Wang, J.P., Matthews, M.L., Naik, P.P., Williams, C.M., Ducoste, J.J., Sederoff, R.R. & Chiang, V.L. (2019). Flux modeling for monolignol biosynthesis. *Current Opinion in Biotechnology*, vol. 56, pp. 187–192.
- Yan, L., Xu, X. & Xia, J. (2019). Different impacts of external ammonium and nitrate addition on plant growth in terrestrial ecosystems: A meta-analysis. *Science of the Total Environment*, vol. 686, pp. 1010–1018.
- Zhao, H., Qu, C., Zuo, Z., Cao, L., Zhang, S., Xu, X., Xu, Z. & Liu, G. (2022). Genome Identification and Expression Profiles in Response to Nitrogen Treatment Analysis of the Class I CCoAOMT Gene Family in *Populus*. *Biochemical Genetics*, vol. 60 (2), pp. 656–675.
- Zhou, X., Wang, A., Hobbie, E.A., Zhu, F., Qu, Y., Dai, L., Li, D., Liu, X., Zhu, W., Koba, K., Li, Y. & Fang, Y. (2021). Mature conifers assimilate nitrate as efficiently as ammonium from soils in four forest plantations. *New Phytologist*, vol. 229 (6), pp. 3184–3194.
- Ziebell, A., Gracom, K., Katahira, R., Chen, F., Pu, Y., Ragauskas, A., Dixon, R.A. & Davis, M. (2010). Increase in 4-Coumaryl Alcohol Units during Lignification in Alfalfa (*Medicago sativa*) Alters the Extractability and Molecular Weight of Lignin. *The Journal of biological chemistry*, vol. 285 (50), pp. 38961–38968.

## SUPPORTING INFORMATION

Additional supporting information can be found online in the Supporting Information section at the end of this article.

**How to cite this article:** Renström, A., Choudhary, S., Gandla, M.L., Jönsson, L.J., Hedenström, M., Jämtgård, S. et al. (2024) The effect of nitrogen source and levels on hybrid aspen tree physiology and wood formation. *Physiologia Plantarum*, 176(1), e14219. Available from: <https://doi.org/10.1111/ppl.14219>